Biol. Cybern. 90, 272–279 (2004)
DOI 10.1007/s00422-004-0470-x

Biological Cybernetics

Signaling contours by neuromorphic wave propagation

Christoph Rasche

Department of Psychology, University of California Santa Barbara, Santa Barbara CA, USA

Received: 29 July 2003 / Accepted: 2 February 2004 / Published online: 31 March 2004

Abstract. We describe a neuromorphic retina that signals a luminance edge as a spike. In a fast process, the luminance profile of the receptor layer determines the membrane potential of the ganglion cells and their individual, adjustable spiking thresholds. In a slower process, a wave-propagation process, the charge of ganglion cells with high membrane potential will propagate toward neighboring cells with low membrane potential and low spiking threshold, thus signaling the edge as a spike. Following that, the signaled edge (or contour) actively propagates across the retinal map. The retinal signal can be used for a contour-integration or a contour-propagation approach.

1 Introduction

1.1 Retina transformations

The retina transforms the luminance profile of our visual environment into a neural code suitable for computation in higher visual areas like the lateral geniculate nucleus (LGN) or the primary visual cortex (V1). This transformation takes place by roughly three functional layers. The first layer, made of the photoreceptors, encodes the luminance intensity by an analog (graded) potential. The second layer, consisting of the horizontal and bipolar cells, performs edge enhancement using also analog potentials (Werblin and Dowling 1969). The third layer, made of ganglion cells, signals a large luminance difference, a high contrast, by generating spikes, which are sent to higher areas (Barlow 1953; Kuffler 1953).

It is generally believed, that the output of such ganglion cells fire a series of spikes, which is transmitted by LGN cells and is read out by the orientation-selective cells in V1 (Hubel and Wiesel 1968), followed by rate-coded networks performing visual computations (e.g. Rolls and Deco 2002). But it has not been shown yet, how specifically this transformation is supposed to happen from a gray-scale image to a rate-firing ganglion cell layer.

An alternative transformation was raised by Thorpe, whose motivation was the observation that visual processing occurs very rapidly (Thorpe et al. 1996). Thorpe suggested that a ganglion cell fires merely a single spike (at least initially), whose exact timing is proportional to the luminance intensity. Higher visual areas would read out the timed spike output of lower areas and generate themselves a timed spike output (Thorpe 1990). Yet again, a specific neuronal implementation of the retinal processing is still outstanding.

We here raise another alternative. Similar to Thorpe's scheme, our model ganglion cells also fire only a single spike, yet only in response to a large luminance difference (contrast). This single spike does not have to be specifically timed. The basis of our process is wave propagation, specifically charge propagation in the ganglion layer. We demonstrate how our contrived transformation performs on gray-scale images, and how its output can be used for our neuromorphic symmetric-axis transform (Rasche 2004), a neuronal implementation of the region-encoding mechanism proposed by Blum (1973).

1.2 Detecting a luminance edge

In a luminance profile, an edge is a large difference between two receptor potentials (Fig. 1a). The problem to be solved by the retinal circuitry is then the following: how is such a large difference between two neighboring receptor potentials signaled by a single spike? This differential should be signaled independent of the absolute luminance level because in a contour profile (of our visual environment) these differences can be at any level and the level itself often varies along a contour. We suggest, that there are two processes at work to solve this problem, a fast and a slow one. In the fast process, a receptor potential determines the

Correspondence to: C. Rasche
(e-mail: rasche@klab.caltech.edu)

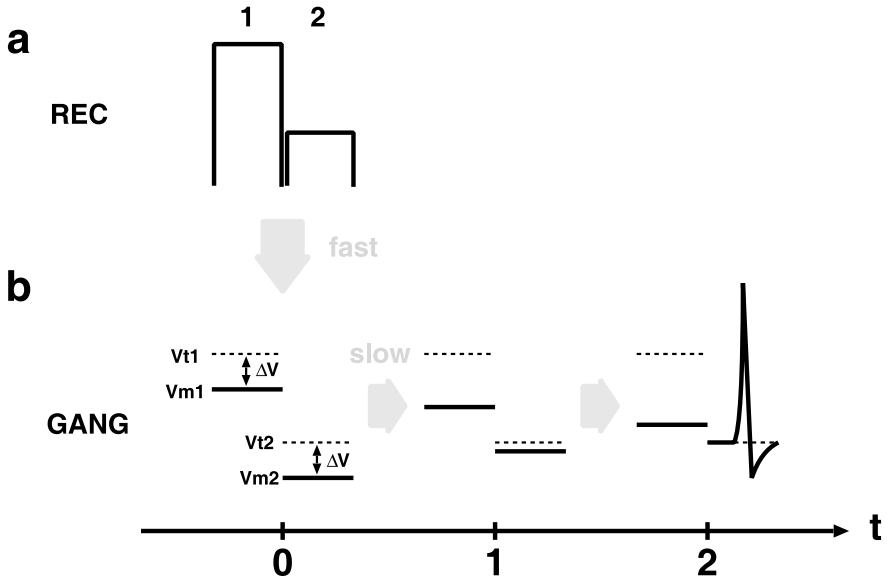

Fig. 1. Receptor potentials and ganglion cell dynamics. **A** Two receptor potentials with large luminance difference. **b** Corresponding two ganglion cells with the membrane potential, V_m, and the spiking threshold, V_t, set above V_m with some fixed voltage offset, ΔV. Both are initially determined by the receptor potential in a fast process. In a subsequent, slower process, the charge will spread (time steps 1 and 2) and V_m will even out (spiking thresholds stay fixed), and cause the neighboring cell to fire, thus signaling the edge

initial membrane potential and the adjustable spiking threshold of its successor (spiking) neuron, which we call ganglion cell now. For reason of simplicity, the second layer (bipolar and horizontal cells) is omitted. The adjustable spiking threshold of the ganglion cells is set above the initial potential with a fixed offset. In the slow process, (Fig. 1b) the charge spreads laterally through the network of connected ganglion cells (time steps 1 and 2). The spiking thresholds stay fixed during this slow process. The charge of a high potential ganglion cell will spread towards its neighboring ganglion cell with a lower potential as well as a lower spiking threshold, and cause it to fire (time step 2). The circuitry and its interactions is shown in Fig. 2. Two compartments of the retina are shown. In the fast process, the photoreceptor (top) charges the ganglion cell node, V_{m1} and V_{m2}, and simultaneously sets the spiking threshold, V_{t1} and V_{t2} of the spiking unit with some fixed voltage offset, ΔV, above the membrane voltages (see grey arrow from photoreceptor output to Spk). In a slow process, the charge of the ganglion cell nodes spreads through the horizontal resistance R_{horiz}. More circuit explanations will be given in the method section.

The motivation for the fast process is that receptors directly determine the membrane potential in their successive ganglion cells, whereas they indirectly determine their adjustable spiking threshold through an extracellular process. For example it has been shown for various brain cell cultures, including retinal preparations, that calcium waves can spread quickly through the gap-junctions of the glia network (Charles 1998). These calcium waves can alter the extracellular calcium concentration rapidly and substantially, and could therefore have a significant effect on the electrical behavior of neurons within short time. The charge propagation is motivated by the fact, that there exist traveling waves in the retina (Jacobs and Werblin 1998).

2 Method

We have software-simulated the processes using simplest dynamics. The fast process is simulated by mere scaling and adding an offset: the gray-scale values of the image are scaled into a range of 0–4.0, representing the individual membrane potentials of each ganglion cell; a value of 0.5, representing the fixed voltage offset (ΔV), is

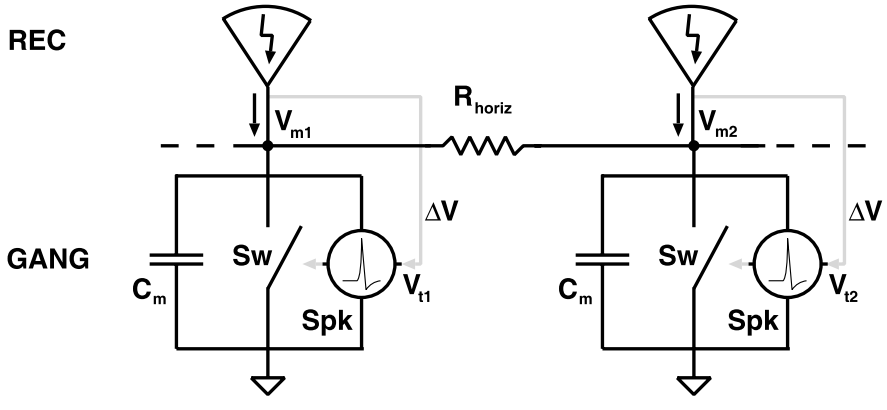

Fig. 2. Circuitry of our retina. Two neighboring nodes (or compartments) are shown. The luminance of the photoreceptors (*top*, REC) charge their corresponding ganglion cell nodes, V_{m1} and V_{m2}, both connected by a horizontal resistance, R_{horiz}. C_m represents the membrane capacitance, Sw is a switch that is activated when a spike occurs, Spk is the spike generating mechanism, whose voltage threshold is determined by the luminance encoded by the photoreceptor (*grey arrow*)

added to each of these potential values, thus mimicking the adjustable spiking thresholds for each individual cell.

The photoreceptors and ganglion cells are arranged in a grid-like array, each one connecting to its eight neighbors. The architecture and operation of this ganglion map is almost identical to the propagation map that we modeled for the simulation of the symmetric-axis transform (Rasche 2004). A ganglion neuron is modeled as a variation of the integrate-and-fire (I & F) unit (Koch 1999), namely as a perfect (or non-leaky) integrator consisting of a membrane capacitance, C_m, a switch, Sw, and a spike generating mechanism, Spk. The membrane capacitance integrates the charge delivered by the horizontal connections (to all of its eight neighbors), R_{horiz}, and the photoreceptor. The spike generating mechanism possesses an adjustable voltage threshold, V_t, triggering a spike. The I & F ganglion cell possesses a refractory property in addition – in order to avoid bounce back of activity – which turns on the switch for a short duration, short-circuiting the node to ground. Instead of simulating the current and voltage dynamics explicitly, we merely model one variable corresponding to the membrane potential, the voltage V_m, of the neuron. When V_m rises above the spiking threshold, V_m is set to a maximum value, E_{Na} – interpreted as the reversal potential for sodium – and stays up there for a short while. Then the refractory period is simulated by setting V_m to a minimum value, E_K – interpreted as the reversal potential for potassium, and stays down there for a short while. The synaptic input from a neighboring neuron (via R_{horiz}) is proportional to the voltage difference. This two-dimensional array of spiking neurons forms an excitable map (or membrane) that can actively propagate a spiking wave.

More formally, the neuronal voltage V_m at location (x, y), at its next step, $t + 1$, of the slow process, is given by its present potential plus the input of its neighboring neurons, $I_n(t)$, and initial external input I_{ph} from the photoreceptor:

$$V_m(x, y, t + 1) = V_m(x, y, t) + I_n(t) + I_{ph} \quad . \tag{1}$$

I_n is the sum of positive membrane differences multiplied by the conductance, g_a, for each of its eight neighboring neurons:

$$I_n(t) = \sum_{k=1}^{8} \max[g_a(V_{m_k}(t) - V_m(t)), 0] \quad . \tag{2}$$

When V_m exceeds the spiking threshold, V_t, a spike of duration d_s is triggered, followed by the refractory period of duration d_r. During the refractory period, the switch is turned on, short-circuiting the node to ground.

The parameters E_{Na} and E_K are set to 5 and 0, respectively. This hypothetical voltage range (from 0 to 5) corresponds to the voltage range used in analog electronic circuits (Mead 1989). The spiking threshold is set by the photoreceptor output during the initial fast process. d_s and d_r are set to 0.6 and 1.2 s, respectively. g_a is set to 0.11. The parameter values are the same as for the propagation map used in our neuromorphic symmetric-axis transform (Rasche 2004).

Shortly after the onset of the slow process – when the wave has propagated into the neighboring neurons – the contours are signaled by a line of spikes. Following that, the spikes continue to propagate across the excitable ganglion map.

3 Results

Figure 3 shows the response of the retina to simple stimuli. In Fig. 3a, the stimulus is a two-dimensional array with zeros and a line of amplitude 3.1373 (already scaled between 0 and 4) in the middle. The corresponding spiking threshold values are 0.5 and 3.6373. After one time step $(t = 1)$, the neighboring neurons have already ignited and therefore signal the line contours. After two time steps $(t = 2)$, the spikes have propagated outward but also backwards toward the line stimulus: all neurons are active for a moment. After three time steps $(t = 3)$, the outward propagation has continued; the neurons that have signaled at $t = 1$ undergo now the refractory period (white 'lines'). After that $(t = 4)$, only the outward-propagating spike wave continues.

In Fig. 3b, the stimulus is a gradient, three adjacent lines of decreasing amplitude. At $t = 1$, the high edge of the gradient is signaled and its flanking sides. The low edge has not yet been signaled because the charge propagation did not raise the neighboring V_m to their individual spiking thresholds. This happens at $t = 2$, when continued outward propagation but also back-propagation from the side helps igniting all the neurons of the gradient. At $t = 3$, the earliest spiking neurons start to undergo the refractory period. From $t = 4$ on, only the outward-propagating spike wave remains.

In Fig. 3c, the stimulus is a block – or four edges. At $t = 1$, all its sides (edges) are signaled. It then follows the inward- and outward-propagation of the spike waves.

It should be emphasized, that for all examples, a backpropagating wave starts, following the initial spikes at $t = 1$ or later.

Figure 4 shows the contour signaling process for two objects, a desk and a chair. The grayscale images are shown in the first row. The second, third and fourth row, show the ganglion spikes after one, two and four time steps. Immediately following the first spikes, the back-propagation starts, which causes the contour to propagate into both directions as for the examples shown in Fig. 3. After two to four time steps, most contours, delineating major surfaces, have been signaled. The high-contrast contours are signaled immediately, followed by low-contrast contours signaled later in time. The bottom row shows the results from the Canny algorithm – a popular computer vision algorithm – for reason of visual comparison (Canny 1986). The algorithm was run on the finest scale (equal to 1) using 0.7 and 0.4 for the high and low threshold, respectively.

Figure 5 shows contour signaling for varying offset values, a low and a high one, $\Delta V = 0.2$ and $\Delta V = 0.8$, respectively. A lower offset value signals more contours

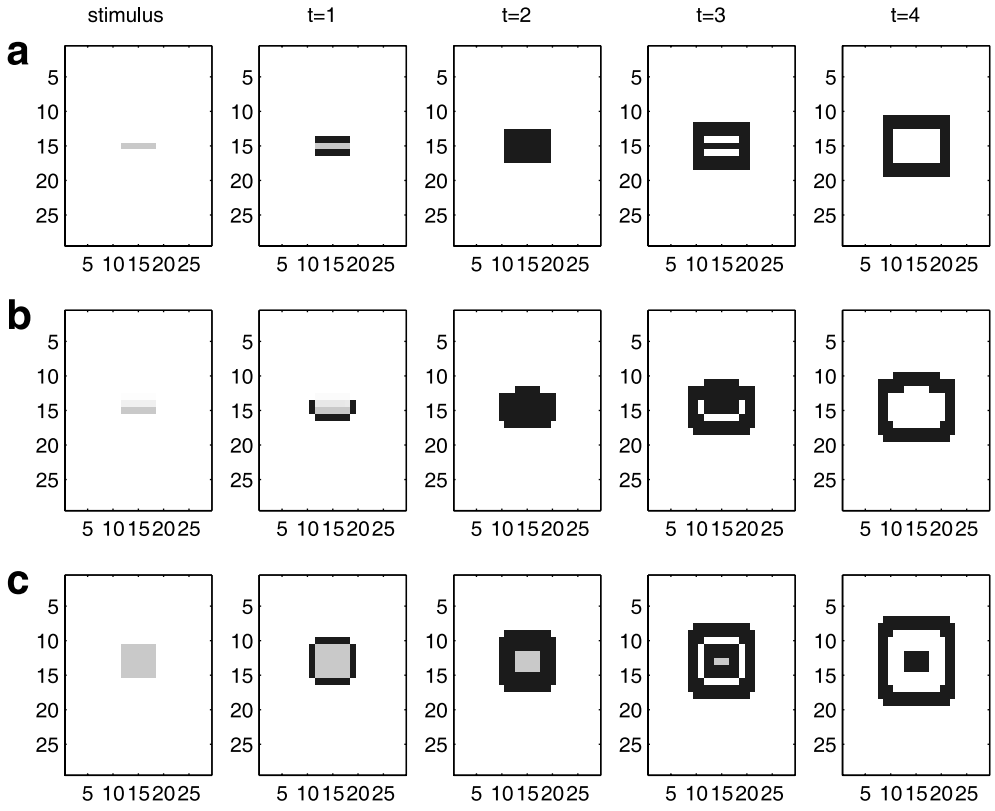

Fig. 3. Contour spikes and subsequent propagation for simple stimuli. **a** Line. **b** Gradient (three *adjacent lines* of decreasing amplitude). **c** Block. The stimuli are shown with inverted gray-scale values for purpose of illustration (zero is *white*, 255 is *black*). Black dots (and *lines*) represent spiking units

and results in slightly faster contour propagation due to the lower spiking threshold. A higher offset value signals high-contrast contours and results in slightly slower propagation due to the high spiking thresholds. For the high voltage offset, there exists no backpropagation because the initial spikes are not able to spread sufficient charge into the neighboring cell with a very high spiking threshold. The offset parameter thus corresponds to the threshold parameter(s) used in the Canny algorithm, or any edge detection algorithm. Its working range is also very large compared to the entire 'voltage range' of 0–5, and makes it therefore a very robust parameter.

The retinal signaling dynamics can be summarized as follows: most contours are signaled in an early phase, followed by a late phase, during which contours propagate into both directions across the retinal map, until they are canceled out due to collision with other contour-propagating waves, or until they have reached the border of the retinal map.

4 Discussion

How can the output of our retina be decoded? There are basically two approaches possible: the classical, popular contour-integration approach and the less pursued contour-propagation approach.

The idea of the contour-integration approach is to integrate line pieces to form an object percept (reviewed in Rolls and Deco 2002). The contour signaled during the early phase can be read out by cortical cells using a single-spike output as response, similar to Thorpe's scheme (Thorpe 1990). Would the late phase, the contour propagation signal, interfere with the contour-integration scheme? Contour-integration may occur so rapidly, due to pure feedforward integration for instance (e.g. Thorpe 1990; Riesenhuber and Poggio 1999), that the late phase is not interpreted anymore and would be overshadowed by the fast, initial percept. Alternatively, the rapid integration in cortex may inhibit the late phase at the thalamic or cortical level via the abundant feedback loops.

The contour-propagation approach is an idea rooting in the Gestaltist's thinking of self-interacting shape (e.g. Koffka 1935). The most influential, computational proposal was made by Blum (1973), which he called the symmetric-axis transform (SAT). He suggested that when two propagating contours collide, that they signal a symmetric point. The loci of symmetric points form a symmetric axis. For a square, the symmetric axis is formed by its two diagonals, which start to evolve in the corners and progress towards the center. The great usefulness of these symmetric axes is, that they express regions (or 2D-space) in a format suitable for high-level vision, namely as a trajectory or vector in a 3D-space with dimensions x, y and time. It is believed that the SAT – or similar region-encoding operations – is carried out in cortical areas (Kovacs and Julesz 1994; Burbeck and Pizer 1995).

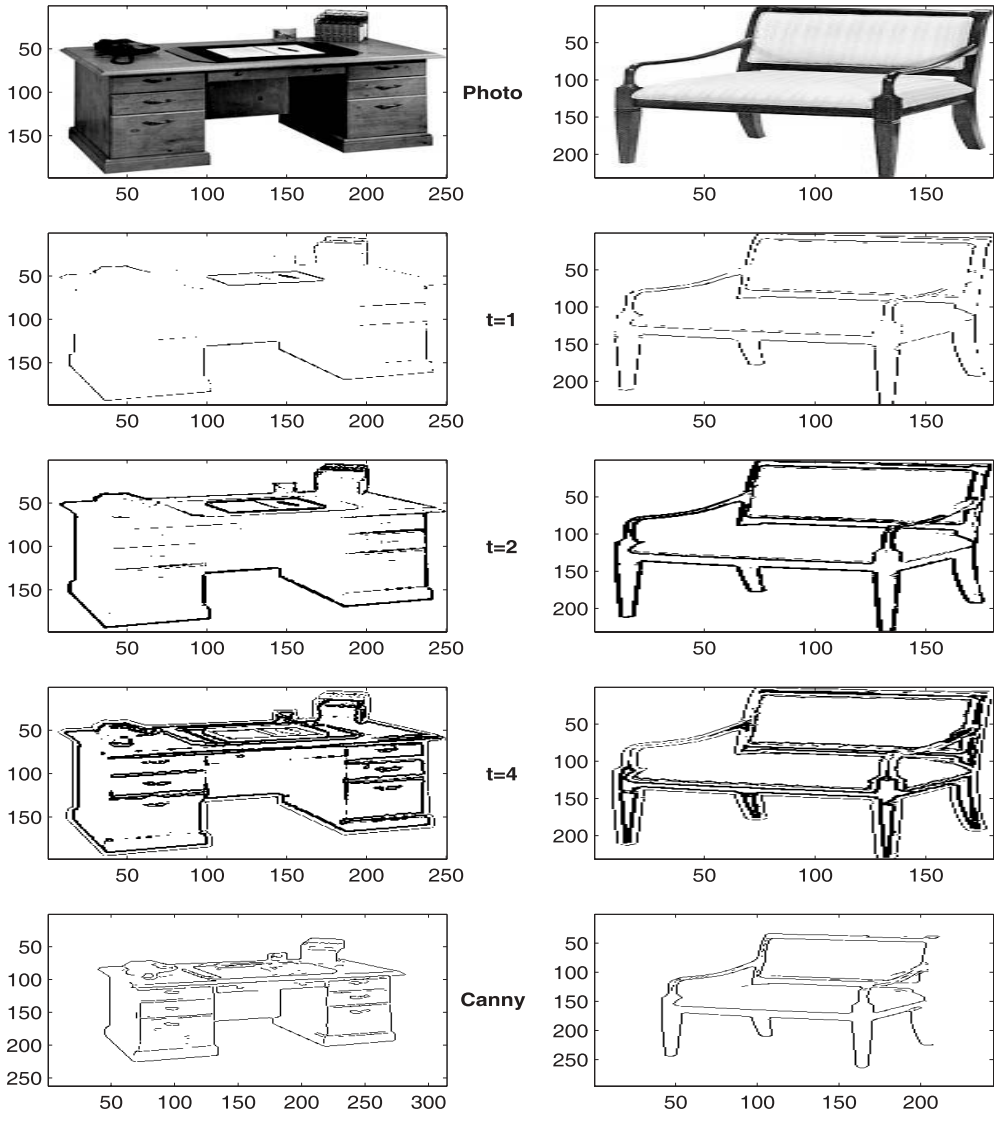

Fig. 4. Contour signaling and propagation. *Top row*: photos. *second, third* and *fourth row*: contour propagation after one, two and three time steps, respectively. $\Delta V = 0.5$. *Black lines* and *dots* represent spikes. *Bottom row*: contours obtained from the Canny algorithm (finest scale)

To simulate the SAT, we used three different layers, a propagation map, orientation columns and a symmetric-axis map (Rasche 2004). The propagation map propagates contours (obtained from a computer vision algorithm) very much like the retinal map. The orientation columns locally detect the orientation of propagating waves. The symmetric-axis map detects when two waves are about to collide and thus signals symmetric points. The orientation columns and the symmetric-axis map are two layers that are rather interpreted as cortical layers. The propagation map however may very well be the retina itself, as we have modeled it here. Our SAT simulation does however work only for propagating waves of width equal one unit, because the orientation columns detect waves of unit width only. Because many waves in the ganglion map are more than one unit wide, their corresponding regions can not be properly encoded. Instead, to demonstrate the value of the retinal output, we keep the retina and the SAT architecture separated and use merely a time-slice of the early-phase retinal output to feed the propagation map of our SAT architecture. Specifically, we have taken the retinal output at $t = 4$ (Fig. 4) as an input to the propagation map of the SAT. The SAT for both objects is shown in Fig. 6. Some of the desktop's regions are not exactly encoded as we humans interpret the objects' regions due to the lack of some contours, but these regions may very well serve as an object hypothesis (Gregory 1997). The simulation should demonstrate that simple neuronal networks – in this case wave-propagating excitable maps – can achieve an enormous amount of visual processing despite the noisy, incomplete contour information inherent in gray-scale images. How the system would operate with the continuous retinal output had to be shown in a separate work.

Our retina model signals contours regardless of the absolute luminance level and uses only one parameter, an offset parameter acting as a contrast threshold. Yet, there may be modifications necessary on our model. For

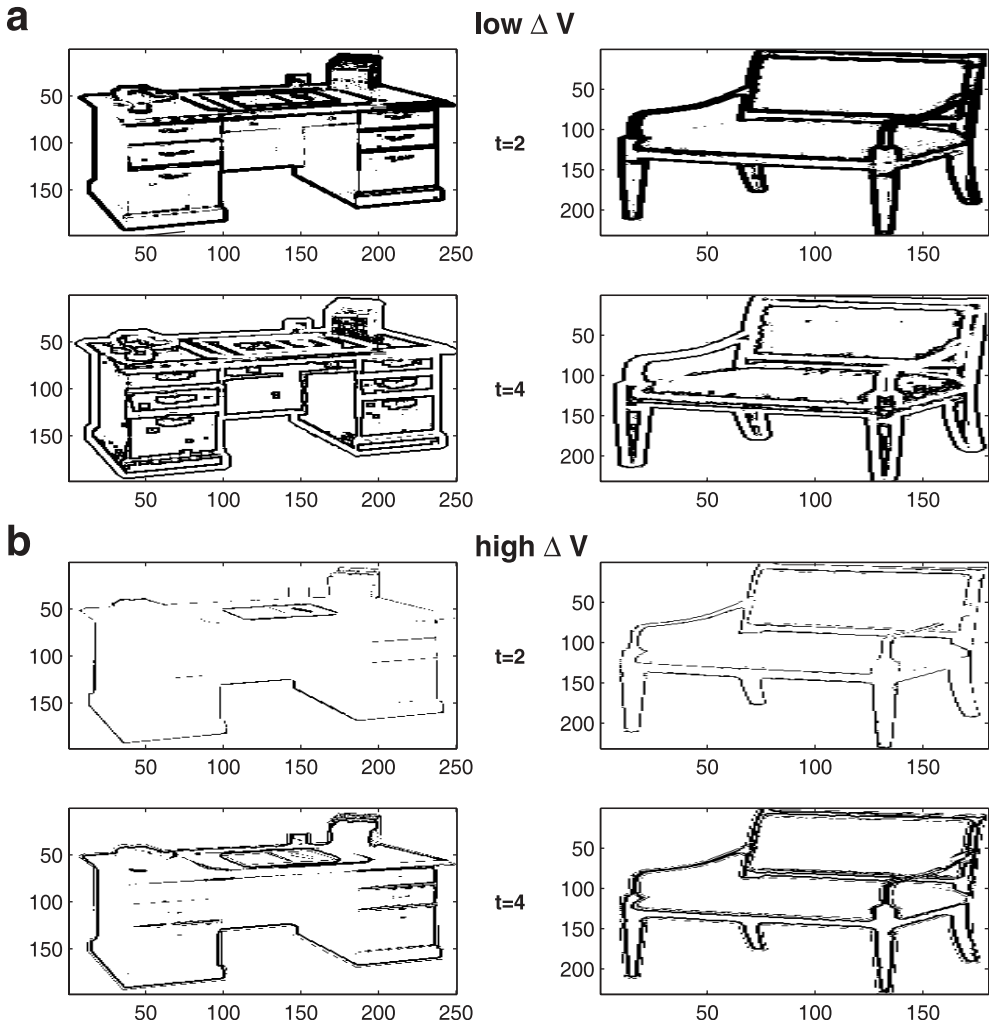

Fig. 5. Effects of varying offset values. Compare also to Fig. 4 where $\Delta V = 0.5$ **a** $\Delta V = 0.2$: more low-contrast contours are signaled. **b** $\Delta V = 0.8$: only high-contrast contours are detected. Time steps 2 and 4 are shown only

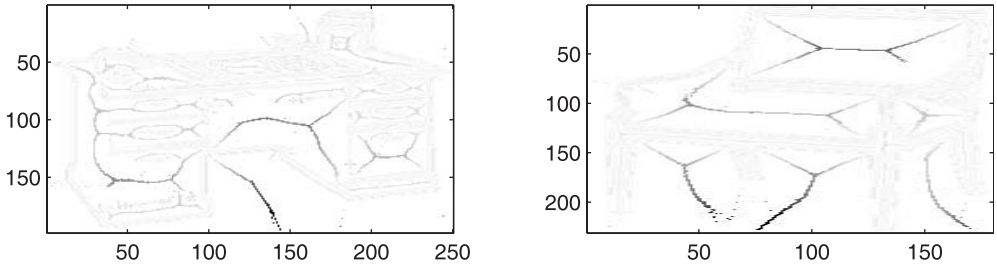

Fig. 6. Encoding regions with the SAT. The spike output at $t = 4$ from Fig. 4 was fed into our neuromorphic simulation of the SAT. Symmetric axes evolve over time, starting in the corner of L features (*light gray*) gradually progressing towards the center of the region (*dark gray*/*black*)

instance, the retina model does not include lateral inhibition, a contour enhancing mechanism, which would help to avoid signaling steep gradients, like the one in Fig. 3b. Because the current retina model works so well on many gray-scale images, we did not see any reason to include it yet, but it may be necessary, if subtle contours had to be detected. Another valuable mechanism that is lacking in our model is adaptation. If for example an image contains low-contrast contours only, then no spikes may be triggered and the offset parameter had to be lowered in order to capture contours. Vice versa, if the image contained a lot of high-contrast contours and for example shadow contours are signaled as well, then the offset parameter may have to be increased.

We regard our proposed retina model primarily as a starting point for a system model. It does not offer a detailed explanation of biophysical events as observed in a real retina. For instance, spontaneous activity – as

observed in real neurons – would trigger traveling waves in our retina model and lead to erroneous contour signaling. The real retina may employ a population code where only a population of neurons may trigger traveling waves and spontaneous activity is swallowed. Our model, however, offers a renewed look at the possible computational involvement of traveling waves. The idea to use traveling waves for neural computation – and not to regard them as accidentally occurring – has hardly been exploited. Blum's symmetric axis transform uses a ''grass-fire'' process, which one can interpret as a traveling wave (Blum 1973). We here use a traveling wave to signal contours. Barch and Glaser apply an excitable membrane – very much like our propagating map – to encode motion: different motion speeds leave traveling waves of characteristic shape on that excitable membrane (Glaser and Barch 1999). Blum also envisioned that traveling waves maybe used to quickly detect coincidences between sensory or motor stimuli, embedded in a model in which the brain would operate as a broadcast-receiver device (Blum 1967).

If the retina model was stimulated with a rapid stream of natural images, then this would trigger many rapidly following propagating waves. It ultimately depended on the real or modeled cortical circuits to read out such rapid signals, whether a contour-integration (e.g. Rolls and Deco 2002) or a contour-propagation approach is at work. Yet, there is also a lower time limit to (human) visual processing of rapidly presented images, which is approximately 150 ms (Potter 1975). Would a smaller object be processed faster in a contour-propagation approach? Not necessarily. The propagation of a shape is often associated with only an inward propagation of its contours like in the case of the SAT. But the outward-propagating shape waves may be decoded as well. It would therefore depend on the nature of cortical shape representation and on how shape is read out. For example it could be the outward-propagating contour wave that triggers recognition and this may occur after the inward-propagating contour waves have collided. In a contour-propagation approach, the stimulation with multiple objects would trigger many waves. Which wave belongs to which object is also a task, whose solution would depend on cortical shape representation and possibly attentional allocation.

The retinal propagation properties may be best compared to the propagation properties measured in the salamander retina. Jacobs and Werblin have shown (Jacobs and Werblin 1998) that, when the salamander retina is stimulated with a bright square on a dark background, two signaling processes take place in the ON-OFF ganglion cells: The first process is the representation of the entire square area by spiking ganglion cells, which develops within 150 ms, followed by the collapse of the ''interior'' of the square after further 50 ms. The second process, is the continued outward-propagation of the remaining ridges of the square, which decays until approximately 350 ms after stimulus onset. The source for the outward-propagating wave can be attributed to either the electrical gap junction coupling of ON bipolar cells (Borges and Wilson 1990; Hare and Owen 1996) or to coupling of horizontal cells (see Jacobs and Werblin 1998 for a more detailed discussion). We relate the following points to these measurements and speculations.

(1) There is no clear sign of a distinct inward propagation in the salamander retina at least not in the ON–OFF ganglion cells. Yet we imagine that there may well be retinal layers in which such an inward propagation could take place.
(2) The main wave (or charge) propagation observed in the real retina seems to take place in the bipolar or horizontal layer. Our model – with only one layer – could be interpreted as a lumped layer of both, the ganglion network and the horizontal connections of the bipolar and horizontal cells.
(3) Visual processing occurs rapidly. A scene gist or an object can be understood in less than 200 ms (Potter 1975; Thorpe et al. 1996; Schendan et al. 1998). Are the observed traveling waves fast enough for such rapid processing? The inner of the square area developed within 150 ms: if the same speed existed in the mammalian retina and if inward-propagation took place in some form, then this maybe just fast enough. Alternatively, there may exist faster traveling waves, as there exist slower traveling waves in other brain regions (Hughes 1995; Prechtl et al. 1997; Wilson et al. 2001; Shevelev and Tsicalov 1997). Fast waves however are difficult to measure experimentally (see Glaser and Barch 1999 for argumentation). Fast waves could rapidly propagate through gap junctions, like the measured waves in the salamander retina apparently do, or the ganglion cells may operate close to the spiking threshold and thus act as quick coincidence detectors.

The proposed retinal processes are conceptually simple enough to be implementable in analog electronic circuits (Mead 1989; Shih-Chii et al. 2002). Several silicon retinae already exist (Mahowald and Mead 1991; Boahen 2002) that signal contours in response to an object moving across their visual field. Our retina would signal contours from a 'still-image' due to the wave 'movement' created within the ganglion map. The resistive network that our ganglion map requires, in particular the horizontal resistance, could be implemented by switched capacitor circuits, which have been used to model dendritic cable properties (Elias 1993; Rasche and Douglas 2001). An important issue in the construction of analog electronic circuits is the robustness of parameters. In an actual electronic implementation, there can be substantial variation amongst transistors leading to inequalities in analog circuit emulation. It is therefore only a hardware realization that would prove, whether the proposed retinal circuits are also technical suitable.

Acknowledgements The study has been carried out in Miguel Eckstein's lab at UCSB, funded by NIH-RO1 53455, NASA NAG 9-1157, NSF 0135118. The author wishes to thank Miguel Eckstein

for generous support, Giacomo Indiveri for comments on the circuit diagram, and the anonymous reviewers for helping to clarify quite a number of discussion points.

References

Barlow H (1953) Action potentials from the frogs retina. J Physiol (London) 1(119): 58–68

Blum H (1967) A transformation for extracting new descriptors of shape. In: Wathen-Dunn W (ed) Models for the Perception of Speech and Visual Form. MIT Press, Cambridge Mass

Blum H (1973) Biological shape and visual science. J Theor Biol 38(2): 205–287

Boahen K (2002) A retinomorphic chip with parallel pathways: encoding increasing, on, decreasing, and off visual signals. Analog Integr Circuits Process 30(2): 121–135

Borges S, Wilson M (1990) The lateral spread of signal between bipolar cells of the tiger salamander retina. Biol Cybern 63(1): 45–50

Burbeck C, Pizer S (1995) Object representation by cores – identifying and representing primitive spatial regions. Vision Res 35(13): 1917–1930

Canny J (1986) A computational approach to edge-detection. IEEE Trans Pattern Anal Machine Intell 8(6): 679–698

Charles A (1998) Intercellular calcium waves in glia. Glia 24(1): 39–49

Elias JG (1993) Artificial dendritic trees. Neural Comput 5: 648–664

Glaser D, Barch D (1999) Motion detection and characterization by an excitable membrane: the 'bow wave' model. Neurocomputing 26–7(216): 137–146

Gregory R (1997) Knowledge in perception and illusion. Philos Trans R Soc Lond Ser B Biol Sci 352(1358): 1121–1127

Hare W, Owen W (1996) Receptive field of the retinal bipolar cell: a pharmacological study in the tiger salamander. J Neurophysiol 76(3): 2005–2019

Hubel D, Wiesel T (1968) Receptive fields and functional architecture of monkey striate cortex. J Physiol (London) 195: 215–243

Hughes J (1995) The phenomenon of traveling waves – a review. Clin Electroencephalogr 26(1): 1–6

Jacobs A, Werblin F (1998) Spatiotemporal patterns at the retinal output. J Neurophysiol 80(1): 447–451

Koch C (1999) Computational Biophysics of Neurons. MIT, Cambridge: Mass

Koffka K (1935) Principles of Gestalt Psychology. Harcourt, Brace, New York

Kovacs I, Julesz B (1994) Perceptual sensitivity maps within globally defined visual shapes. Nature 370(6491): 644–646

Kuffler S (1953) Discharge patterns and functional organization of mammalian retina. J Neurophysiol 16: 37–68

Mahowald M, Mead C (1991) Silicon retina. Sci Am 264(5): 76–82

Mead CA (1989) Analog VLSI and Neural Systems. Addison-Wesley, Reading, MA

Potter MC (1975) Meaning in visual search. Science 187(4180): 965–966

Prechtl J, Cohen L, Pesaran B, Mitra P, Kleinfeld D (1997) Visual stimuli induce waves of electrical activity in turtle cortex. Proc Natl Acad Sci USA 94(14): 7621–7626

Rasche C (2004) A neuromorphic simulation of the symmetric axis transform. Under review

Rasche C, Douglas R (2001) Forward- and backward-propagation in a silicon dendrite. IEEE Trans Neural Netwo 12(2): 386–393

Riesenhuber M, Poggio T (1999) Are cortical models really bound by the binding problem? Neuron 24(1): 87–93, 111–125

Rolls E, Deco G (2002) Computational neuroscience of vision. Oxford University Press, New York

Schendan HE, Ganis G, Kutas M (1998) Neurophysiological evidence for visual perceptual categorization of words and faces within 150 ms. Psychophysiology 35(3): 240–251

Shevelev I, Tsicalov E (1997) Fast thermal waves spreading over the cerebral cortex. Neuroscience 76(2): 531–540

Shih-Chii L, Kramer J, Indiveri G, Delbrueck T, Douglas R (2002) Analog VLSI: Circuits and Principles. MIT Press, Cambridge, MA

Thorpe S, Fize D, Marlot C (1996) Speed of processing in the human visual system. Nature 381: 520–522

Thorpe SJ (1990) Spike arrival times: a highly efficient coding scheme for neural networks. In: Eckmiller R, Hartmann G, Hauske G (eds) Parallel Processing in Neural Systems and Computers, pp 91–94, Elsevier Science Publishers

Werblin F, Dowling J (1969) Organization of retina of mudpuppy necturus maculosus 2. intracellular recording. J Neurophysiol 32(3): 339

Wilson H, Blake R, Lee S (2001) Dynamics of travelling waves in visual perception. Nature 412(6850): 907–910